

Successful Encapsulation of Hydrophilic Drug in Poly (Lactic Acid)/Chitosan Core/Shell Nanoparticles

Karine Cappuccio de Castro^{1,2*}, Rodolfo Debone Piazza³, Rodrigo Fernando Costa Marques³ and Maria Gabriela Nogueira Campos¹

¹Federal University of Alfenas, Institute of Science and Technology, Graduate School of Materials Science and Engineering, Poços de Caldas-MG, Brazil

²State University of Campinas, Faculty of Chemical Engineering, Department of Materials Engineering and Bioprocess, Cidade Universitária Zeferino Vaz, Campinas-SP, Brazil

³UNESP - São Paulo State University, Institute of Chemistry, Araraquara-SP, Brazil

*Corresponding author

Karine Cappuccio de Castro, Federal University of Alfenas, Institute of Science and Technology, Graduate School of Materials Science and Engineering, Poços de Caldas-MG, Brazil, E-mail: cappuccio.karine@gmail.com

Submitted: 05 Apr 2019; Accepted: 12 Apr 2019; Published: 14 May 2019

Abstract

Nanotechnology may be an alternative to overcome the limitations of conventional treatments, through the creation of nanostructured devices capable of directing the antimicrobial to the affected tissue. In this paper, polylactic acid (PLA)/chitosan (CH) nanoparticles were synthesized for controlled release of gentamicin (hydrophilic drug) through the simple emulsification-solvent evaporation method. The results suggest the successful formation of PLA/CH core-shell nanoparticles. Zeta potential analysis showed that the particles have positive surface charges, which is attractive for cell adhesion and suggest the presence of CH in the shell. The burst release observed at the first 6 hours was due to the gentamicin bonded in the CH shell. However, after 24 hours, the system resumed releasing, confirming the interaction and release of gentamicin from the PLA core. The antimicrobial assay indicated inhibition of growth of *Staphylococcus aureus*, confirming the effectiveness of the encapsulation and release of gentamicin from PLA/CH nanoparticles.

Keywords: Nanoparticles Chitosan, Poly (Lactic Acid), Drug Delivery, Gentamicin

Introduction

Bacterial infections, such as mastitis, cause painful inflammation accompanied by leukocyte and serum protein diffusion from the blood to the infected site [1-2]. Traditional antibiotic treatment may be painstaking, besides it can lead to failure in infection control or delay in healing, since the drug dosage is imprecise and delivered discontinuously. Moreover, the antibiotic cannot reach some cellular compartments, being blocked by the organism's defense cells. In this context, new nanostructured drug delivery systems have been developed with potential ability to enter defense cells through the process of phagocytosis and control the continuous gentamicin (GEN) releasing for treatment of this disease.

Biodegradable Nanoparticles (NPs) are under intense investigation due to their potential application in targeted drug delivery [3-5]. Some polymers have aroused greater interest due to their applicability potential, and their excellent biodegradability and biocompatibility properties [5]. In addition, polymeric nanoparticles are structurally stable and can be synthesized with greater size distributions control. Polymers such as Chitosan (CH) and Polylactic Acid (PLA) have

gained prominence for this purpose [6-7].

CH is a natural polymer that becomes a polycation at acid pH with mucoadhesive characteristics, increasing its affinity for biological membranes [5,6]. CH ability to be positively charged also allows an increase in the residual time of the drug at the absorption site and can promote increased bioavailability that favors its use as nanoparticles [6]. Polylactic acid, in turn, is one of the aliphatic polymers can be obtained from renewable sources and is used for the production of biocompatible and bioabsorbable devices [7-9]. This polymer has high crystallinity and low hydrophilicity which reduces its degradation rate [10-11]. Another important factor is that PLA can generate negative charges on the surface, which favors its interaction with chitosan during nanoparticles synthesis [12].

PLA/CH nanoparticulate systems for drug delivery have been extensively studied in the literature, however, the synthesis of such systems using the emulsification-solvent evaporation method, are only used to transport hydrophobic drugs [5,11,13-17]. There are few reports of these devices in the transport of hydrophilic drugs, and those that exist use another route of synthesis, since this is a consolidated route in the encapsulation of hydrophobic drugs [10,18,19].

Therefore, the synthesis of PLA/CH core-shell nanoparticles prepared by emulsion-solvent evaporation methodology was investigated, for potential application as a gentamicin delivery system in the treatment of infections. The results also provide a new route for the use of PLA/CH nanoparticles as release vehicles for hydrophilic drug, which had not yet been reported in the literature, according to our knowledge.

Materials and Methods

Synthesis of Nanoparticles

The samples were prepared by an oil in water emulsification (O/W) followed by ultrasonic solvent evaporation, adapted from Dev et al. (2010) [10]. 37.5 mg average molecular weight chitosan (Sigma-Aldrich, USA) was solubilized in 30 mL 0.1% (v/v) acetic acid solution (Proquímios, Brazil). One drop of Tween80[®] (Fagron, Brazil) was added to each 100 ml of acetic acid solution (aqueous phase). Subsequently, 50 mg PLA (M_n 116848, polydispersity: 1.67) was dissolved in 5 mL dichloromethane (DCM) (organic phase). Afterwards, all organic phase was poured into the aqueous phase (sample 1: 0.75, that is, proportion of 1PLA: 0.75CH). For samples 1:0.50 and 1:0.25 it was varied only the amount of chitosan. The solutions were then mixed and shaken in a Turrax (model T10 Basic, IKA) at a rotation of 30,000 rpm for 10 minutes. The resultant suspension was placed on an ultrasonic probe (Hielscher) for 30 minutes (3s on/ 3s off cycle) and with amplitude of 40%. The suspension was centrifuged (7500 RPM, 40 min - Centrifuge Model 5804R, Eppendorf) and filtered through a syringe filter (0.45µm) and freeze-dried for further analysis.

Synthesis of Gentamicin loaded PLA/CS nanoparticles

The hydrophilic drug encapsulation was done using the same methodology described in the previous item, with the addition of the gentamicin solution in the aqueous phase. Aqueous gentamicin solution (86µm) was first poured into a polymer solution (37.5 mg of CH dissolved in 30 ml of 0.1% acetic acid solution containing Tween80[®]) to form emulsion. Sequentially 50 mg of PLA were dissolved in 5 ml of dichloromethane and the solution formed was rapidly poured into the emulsion containing the antibiotic. The mixture was stirred to form an emulsion, and then sonicated, under the same conditions used to prepare the nanoparticles in the absence of gentamicin.

Particle Size Distribution

Average diameter and particle size distribution data were collected from the nanoparticles suspensions by Dynamic Light Scattering (DLS) technique (ZetasizerNanoseries, model ZS90, Malvern Instrument).

Zeta Potential and Colloidal stability at various pH's

Zeta potential data was collected (Zetasizer Nano series, model ZS90, Malvern Instrument). In addition, the effect of pH in the range 2.0 – 10.0 on the zeta potential measurements were also analyzed. Nanoparticles (9.0mg) were suspended in 30 mL of distilled water under stirring on an ultrasonic probe for 2 minutes. In all instances, 0.01M NaOH solution was used to increase the pH and a 0.01M HCl solution was used to decrease the pH.

Scanning Electron Microscopy (SEM)

Morphology of freeze-dried nanoparticles dispersed in deionized water was analyzed by SEM (model Leo 440i - LEO Electron Microscopy/Oxford). 5µL of each sample was dripped onto a silicon

port, dried overnight and covered with 200Å of gold (Sputter Coater EMITECH, model K450).

Fourier Transform Infrared Spectroscopy (FTIR)

Infrared spectra were collected on a Spectrometer (Perkin Elmer-Frontier) and recorded from 500 to 4000 cm⁻¹. The inter- and intramolecular interactions between the polymers were evaluated by the presence of characteristics functional groups of CH and PLA in the nanoparticles.

Thermogravimetric analysis (TGA)

Determination of weight loss of PLA/CH nanoparticles, CH and PLA was performed on a Differential Scanning Calorimeter (NETZSCH - Model STA 449 F3Jupiter) under nitrogen atmosphere from 37°C to 800°C at a heating rate of 10°C/min and N₂ flow rate of 20 cm³/min.

Drug encapsulation efficiency

The obtained GEN loaded nanoparticles suspension was centrifuged at 10000 RPM for 25 min (Centrifuge HT-MCD-2000). The supernatant was diluted twice and 1 ml of it was subjected to the colorimetric method described by Frutos et al. (2000). The solution was measured by UV spectrophotometer (Cary 60, Agilent Technologies) at the wavelength 400 nm and the weight of drug was calculated by using calibration curve. The efficiency of encapsulation was calculated by Eq. 1:

$$\text{Encapsulation efficiency} = \frac{\text{Weight of gentamicin drug in nanoparticles}}{\text{Weight of gentamicin drug initially}} \times 100\%$$

In vitro drug release

The *in vitro* drug release assay was carried out on all formulations. 4 mg of each sample were suspended in 1 ml of distilled water and placed in a dialysis membrane bag with a molecular cut-off of 3.5kDa. Samples were immersed into 10 ml of PBS buffer (pH=7.4). The entire system was kept at 37°C in an incubated shaker at 120 rpm. After a predetermined period, 1 ml of the medium was collected and the concentration of gentamicin was evaluated by UV spectrophotometer (Cary 60, Agilent Technologies) at 400 nm. In order to maintain the original volume, once collected, 1ml of medium was replaced with same volume of fresh PBS buffer. This assay was repeated three times.

Evaluation of antimicrobial activity by the disk diffusion method

Colonies of *Staphylococcus aureus* were recovered in Brain Heart Infusion (BHI) broth at 37°C for 24 hours. The antimicrobial susceptibility was evaluated by the disc diffusion method, according to CLSI recommendations (2009a) and with the methodology described by Almeida et al. (2014) [20-22]. Here, sterile filter paper discs received a 10 µL aliquot of each nanoparticle suspension (4 mg/mL) to be tested, and then the disk was applied with sterile forceps onto a Petri dish containing Mueller-Hinton agar (MH), previously inoculated with the microorganism. The inhibition zone around the discs were measured after 24 hours of incubation at 37°C.

Evaluation of antimicrobial activity by the micro-dilution technique

Staphylococcus aureus was cultured into BHI broth in screw capped tubes and incubated at 37°C for 24 hours. The antimicrobial screening was performed in clear 96-well plates containing 100 µL of BHI liquid medium in each well except the first well. The samples were successively diluted in each row. Gentamicin solution was used

as positive control and water as negative control. Broth only was also tested to check for contamination. 100 μL of bacterial solution was added to each well, except to the broth only ones. The final volume of each well after the dilution procedure was 200 μL . The plate covered was incubated for 24 hours at 37°C. After this, 10 μL of a 0.01% aqueous solution of sodium resazurin was added to each of the wells. After 1 hour, the visual reading of the results was done, in which blue characterizes bacterial inactivity, and pink color refers to bacterial metabolic activity.

Results

Fig. 1 shows the results on PLA/CH nanoparticles unloaded and loaded with gentamicin. The average particle size is in the range of 150–400 nm (Fig. 1).

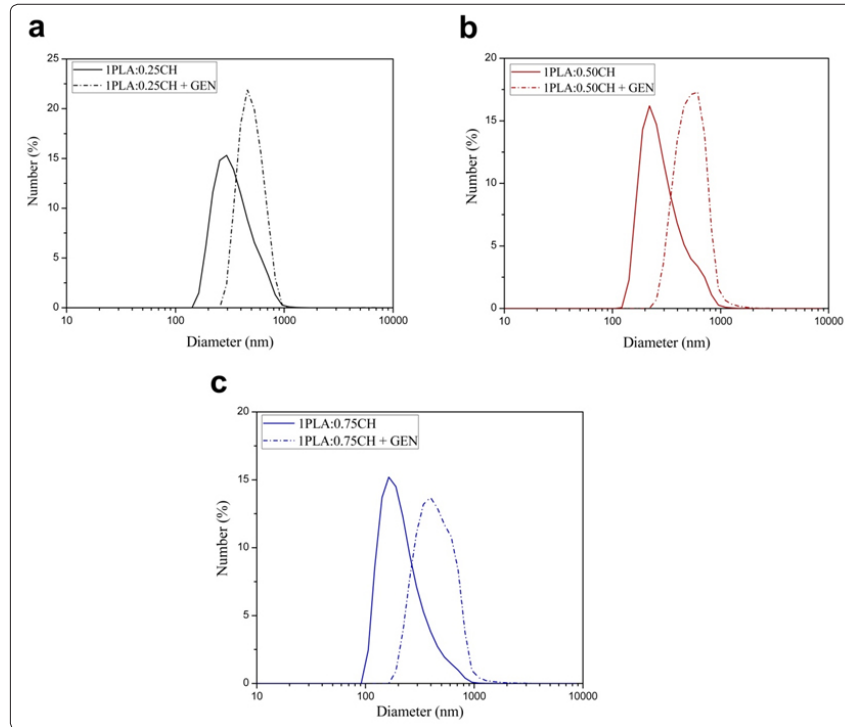


Figure 1: Comparison of particle size before and after gentamicin (GEN) encapsulation. PLA:CH ratio: (a) 1:0.25 (b) 1:0.50 (c) 1:0.75.

From the results of zeta potential listed in Tab. 1, it is found that PLA/CH nanoparticles have positive surface charge of about 23–35 mV. PLA/CH nanoparticles loaded with gentamicin also have positive charge of about 14–26 mV. The positive charged surface of PLA/CH nanoparticles is probably due to the cationic characteristic of CH, and was reported in other studies with chitosan nanoparticles [5, 22]. This may suggest that a PLA/CH core-shell structure has been formed. The decrease on the nanoparticles surface charge after gentamicin loading may be due to the dual gentamicin interactions with CH positive charges and PLA negative charges.

Table 1: Zeta Potential measurements and encapsulation efficiency.

Nanoparticles*	Zeta Potential (mV)	GEN Loaded Nanoparticles*	Zeta Potential (mV)	EE (%)
1:0.75	31±4	1:0.75	25±1	66.7
1:0.50	36±1	1:0.50	26±1	68.7
1:0.25	24±1	1:0.25	15±1	75.8

*pH=7.4

The colloidal stability was evaluated at various pH's. Zeta potential results showed positive charged nanoparticles in a wide pH range (2 to 7), indicating that nanoparticles were stable at physiological conditions (Fig. 2). Nevertheless, from pH 8 to 10, zeta potential was reduced, compromising particle stability in the suspension. In addition, Zwitterionic behavior is reached around pH 10. This can be attributed to the balance of charges of both CH and PLA polymers, as well as GEN, in equilibrium with hydroxyl groups at this pH.

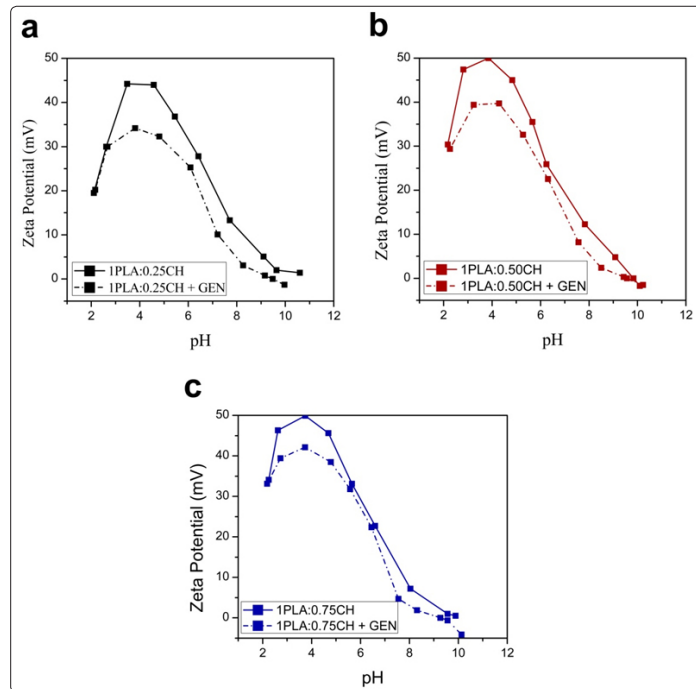


Figure 2: Colloidal stability of freeze-dried nanoparticles dispersed in water: Zeta potential values of nanoparticles unloaded and loaded with gentamicin (GEN) at different pH's. PLA: CH ratio: (a) 1:0.25 (b) 1:0.50 (c) 1:0.75

Morphological characterization of nanoparticles was carried out by SEM. Fig. 3 shows the SEM images of unloaded and gentamicin loaded PLA/CH nanoparticles.

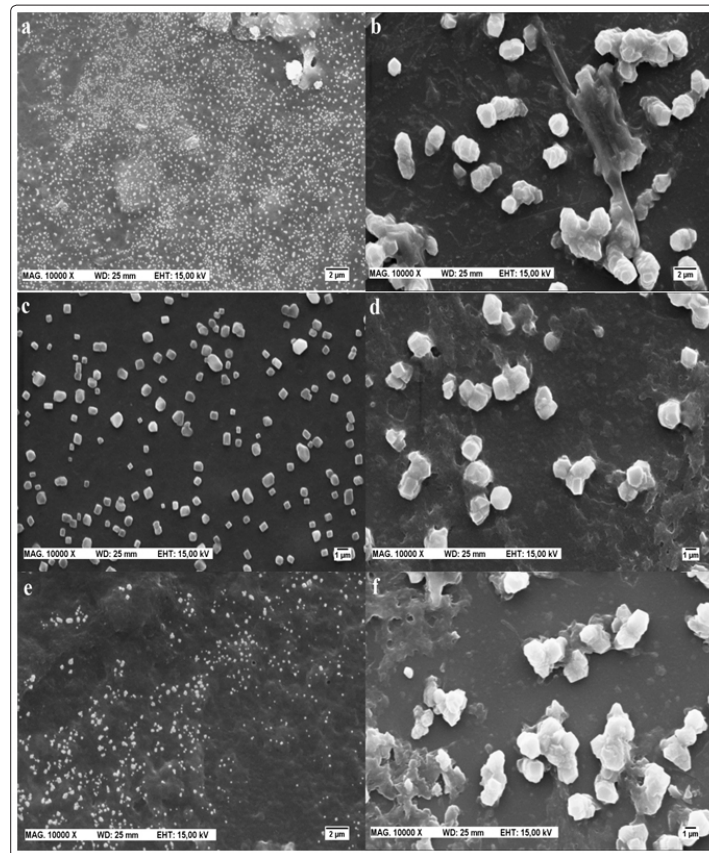


Figure 3: SEM images of nanoparticles resuspended in water after freeze-drying. PLA: CH ratio: (a) 1:0.25 (b) 1:0.25 + GEN (c) 1:0.50 (d) 1:0.50 + GEN (e) 1:0,75 (f) 1:0.75 + GEN

A prior assessment in the FTIR spectra (Fig. 4a) of PLA/CH nanoparticles showed the characteristic peaks of PLA and CH individually. The characteristic peaks of CH, PLA and GEN were identified in the spectra of PLA/CH nanoparticles and PLA/CH nanoparticles loaded with gentamicin.

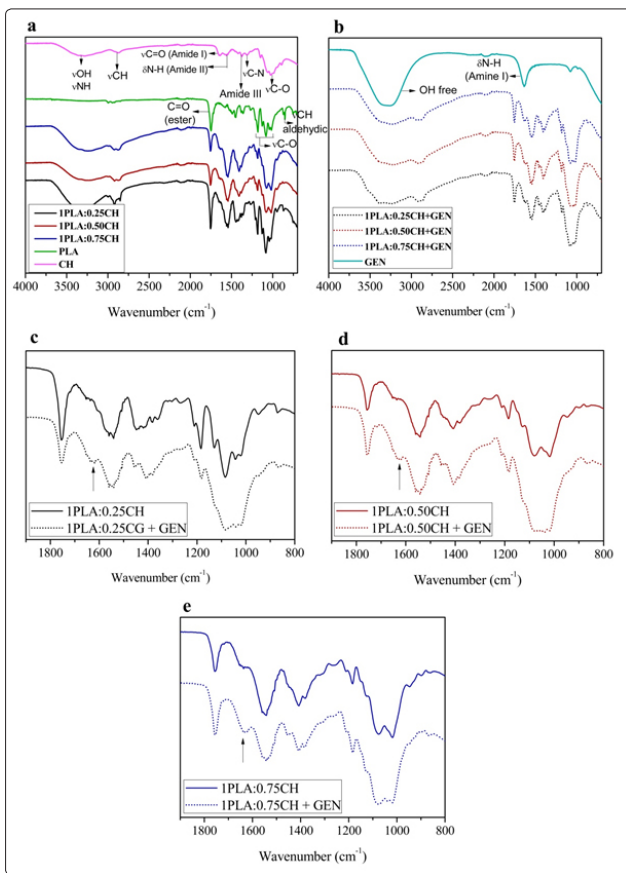


Figure 4: FTIR Spectra (% Transmittance): (a) Nanoparticles and synthesis components (b) Loaded nanoparticles and gentamicin. Comparison between unloaded and loaded nanoparticles - PLA: CH ratio: (c) 1: 0.25 (d) 1: 0.50 (e) 1: 0.75

Thermal properties of PLA, CH and PLA/CH nanoparticles were studied by TGA analysis (Figure 5). Results show that nanoparticles have lower thermal stability when compared to their individual components. In addition, it is possible to observe that the thermal stability is decreased even further gentamicin encapsulation.

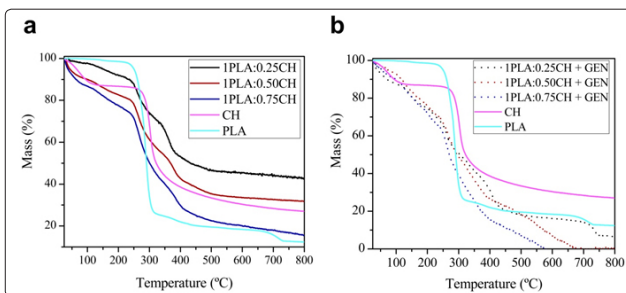


Figure 5: TG curves of PLA, CH, and PLA/CH nanoparticles: (a) PLA/CH nanoparticles (unloaded) (b) PLA/CH nanoparticles loaded with gentamicin.

In order to explore the possibility of using PLA/CH nanoparticles as hydrophilic drug carriers, gentamicin was used as a model drug. The percentage of gentamicin encapsulated in each PLA/CH nanoparticle formulation is shown in Tab. 1. In addition, the *in vitro* study of GEN release is presented in the Fig. 6.

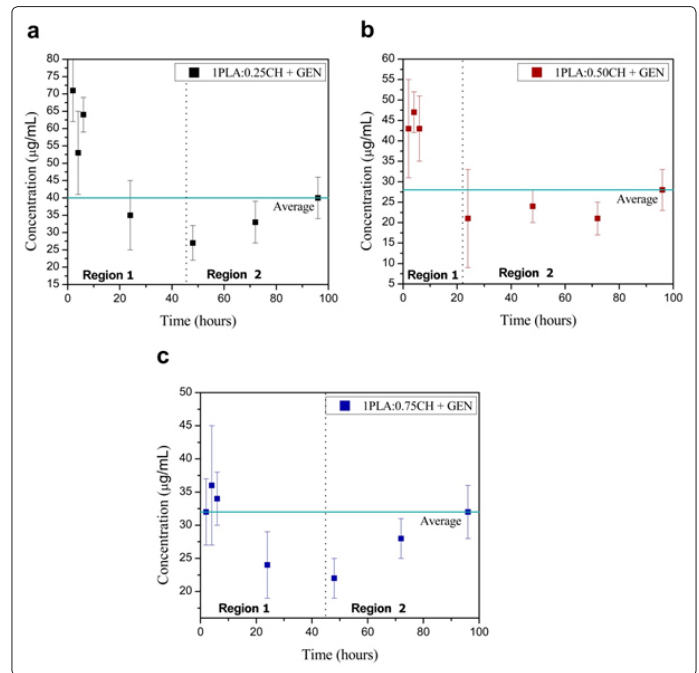


Figure 6: Cumulative release profile of PLA/CH nanoparticles loaded with gentamicin in the 96 hour period. PLA: CH ratio: (a) 1:0.25 (b) 1:0.50 (c) 1:0.75

Note: All concentrations should be multiplied by the dilution factor ($f = 10$).

In addition to *in vitro* release studies, the activity of gentamicin against *Staphylococcus aureus* was evaluated by the disk diffusion method. As expected, growth-inhibition zones were only observed around the disks treated with gentamicin-loaded nanoparticles (Fig. 7). This indicates the incorporation of the antibiotic into the nanoparticles and their capability to release gentamicin.

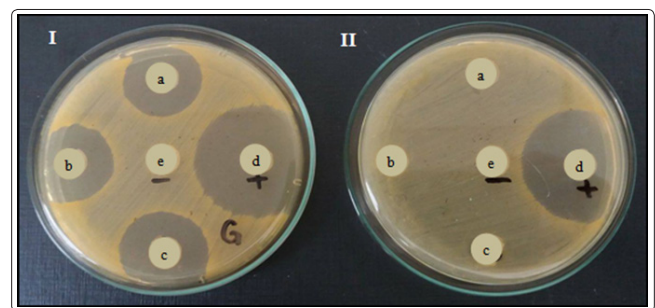


Figure 7: Antimicrobial activity of nanoparticles against *Staphylococcus aureus*. I - Gentamicin-loaded nanoparticles: PLA: CH ratio (a) 1:0.75 (b) 1:0.50 (c) 1:0.25 (d) Positive Control (e) Negative Control. II - Nanoparticles without gentamicin: (a) 1:0.75 (b) 1:0.50 (c) 1:0.25 (d) Positive Control (e) Negative Control

Another experiment was carried out to screen the antimicrobial activity of nanoparticles against *Staphylococcus aureus* in liquid

culture media. Concentration of gentamicin on gentamicin-loaded PLA/CH nanoparticles that visually inhibited bacterial activity are presented on Tab. 2.

Table 2: Concentration of gentamicin on gentamicin-loaded PLA/CH nanoparticles that visually inhibited bacterial activity

Gentamicin Concentration ($\mu\text{g/mL}$)		
1:0.25 + GEN	1:0.50 + GEN	1:0.75 + GEN
1.32	0.99	0.86

Bacterial activity was evidenced by color change after addition of resazurin sodium to the wells. As the concentration of gentamicin increased, the coloration assumed darker shades, indicating inhibition of bacterial activity. The red rectangles delimited in the plate rows indicate where inhibition of bacterial activity was observed (Fig.8).

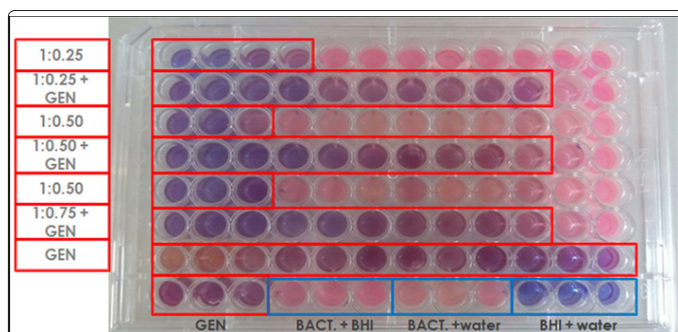


Figure 8: 96 well plate used in the microdilution experiment after incubation with resazurin to visualize bacterial activity.

Note: Bacterium (BACT.), Gentamicin (GEN) and Brain Heart Infusion (BHI).

Discussion

DLS analysis showed that gentamicin-free particles were more monodisperse than gentamicin-loaded nanoparticles (Tab. 1), which was confirmed by SEM images (Fig. 3). Gentamicin-loaded nanoparticles also showed agglomeration points (Fig. 3), which justified larger average size for this system when compared to the system without the drug (Fig. 1). SEM micrographs of nanoparticles prior to freeze drying process (data not shown) showed that gentamicin has a structural effect on the nanoparticles, decreasing the average diameter and reducing the polydispersity of the particles.

Size of nanoparticles is important because it is related to the stability, cellular uptake, bio-distribution and drug release [15]. Nanoparticles with diameters greater than 300 nm are known to induce phagocytosis and macropinocytosis due to the triggering of opsonization of the particles. This mechanism allows the removal of foreign particles from host cells in excess or damaged within the organism [23-24]. On the other hand, particles smaller than 300 nm are more suitable for adhesion and surface cellular interaction [25]. Particle size distribution (Fig. 1) shows good application for the two sequences, which is interesting for intra and extracellular action on the site affected by bacterial infection.

In the nanoparticle synthesis process, chitosan interacts to PLA surface due to strong intermolecular hydrogen bonds, which makes nanoparticles surface charges positive (Tab. 1). Moreover, the amino groups in CH molecule have higher ionic conductivity which

contributes to the increase in the charge density of the polymer during the preparation process [13,15,26,27]. Zeta potential reduction with the antibiotic encapsulation occurred because there was less availability of amino groups on the nanoparticles surface due to the gentamicin-chitosan interaction, which indicates the formation of core-shell nanoparticles in which the nucleus composed of PLA is covered by chitosan. This hydrophobic-hydrophilic biodegradable nanoparticle system can serve as drug carriers.

The pH of as synthesized nanoparticle suspension was around 4.0. After freeze-drying and redispersion in distilled water, the suspension pH was 7.0 (close to physiological conditions). In addition to pH effect, freeze-drying process also facilitates nanoparticles' storage and increases their shelf-life that are important parameters for biomedical application. At pH 4.0, it is expected greater interaction of gentamicin with PLA (hydrophobic character) than chitosan (hydrophilic character) due to the protonation (positive charge) of CH and GEN amine groups that causes charge repulsion between these molecules. This fact justifies greater encapsulation efficiency of gentamicin in samples with less amount of chitosan (Tab. 1). It is noteworthy that the slight acidic pH surrounding bacterial infection will cause CH amine groups protonation, which enhances mucoadhesive property of nanoparticles and increases their retention in the site of application [28-31].

FTIR analysis of nanoparticles and their individual components are presented in Fig. 4. The peaks at 1582 and 1540 cm^{-1} correspond to the amide group of CH. The multiple peaks at 870 and 1190 cm^{-1} are the result of polysaccharide structure of CH [11,32-33]. The peak at 1322 cm^{-1} is the characteristic band of CH₃ symmetrical deformation mode. The peaks between 3200 and 3350 cm^{-1} are due to the hydrogen bonded -OH group. The peak around 1789 cm^{-1} is attributed to carboxylic groups on the PLA side chains. The peak present in the gentamicin drug spectrum at 1632 cm^{-1} was due to N-H (Fig. 4b) [34]. In addition, the peak shifts between 1000 and 1100 cm^{-1} show the interaction between polymers and drug (Fig. 4c, d and e). This also confirms the drug was incorporated into the polymeric nanoparticles.

TGA analysis shows that CH has a two-stage degradation pattern in TG curves (Fig. 5), which may be attributed to the moisture losses and thermo-degradation of the CH chains [9,35-36]. On the other hand, PLA presents a one-stage of thermo-degradation corresponding to the degradation of the hydrocarbon chain.

The nanoparticle sample with the lowest amount of CH (1 PLA: 0.25CH) showed higher thermal stability in the initial phase of the analysis, indicating higher prevalence of PLA in the synthesized material. This initial phase is a result of sample moisture loss. As PLA is hydrophobic, it is possible that this sample retains less moisture.

Drug encapsulation efficiency was higher for sample 1PLA:0.25CH (75.8%) (Tab.1). The lower encapsulation efficiency presented by 1PLA:0.50CH (68.7%) and 1PLA:0.75CH (66.7%) samples can be explained by the lower amount of PLA available for interaction with the drug, since greater amount of chitosan in the formulation causes competition between chitosan and gentamicin for binding with the -OH groups of PLA.

The profile of gentamicin release (Fig. 6) showed two stages. In the first 6 hours of release, a dilution process occurred (Region 1) and the gentamicin bound to chitosan on the surface of the nanoparticle (shell) was released. After 24 hours, gentamicin concentration started to increase again (Region 2), indicating that the antibiotic bound to PLA in the core of the nanoparticle was being released.

The capability of nanoparticles to delivery gentamicin and inhibit *Staphylococcus aureus* growth was confirmed by the presence of inhibition zones around the disks treated with gentamicin-loaded nanoparticles (Fig. 7). In addition to disk diffusion assay (agar), antimicrobial activity of nanoparticles was also evaluated against *Staphylococcus aureus* using the resazurin assay in liquid culture media. Bacterial activity was analyzed by color change in the media after resazurin addition, and the concentration of gentamicin on the nanoparticles that visually inhibited bacterial activity was determined (Tab. 2). The results on gentamicin concentration were in accordance with Literature that reports Minimal Inhibitory Concentration (MIC) and Minimal Bactericidal Concentration (MBC) of gentamicin against *Staphylococcus aureus* as 0.5 µg/mL and 2 µg/mL, respectively [37]. Nanoparticles without gentamicin at high concentration also inhibited bacterial activity, possibly due to chitosan antimicrobial properties.

Acknowledgements

The authors thank the Department of Physical Chemistry of the Institute of Chemistry of the São Paulo State University-UNESP and to the Graduate School of Science and Materials Engineering at the Federal University of Alfenas-UNIFAL.

Funding: This work was supported by CAPES, CNPq and FAPEMIG.

References

1. Fan J, Zeng Z, Mai K, Yang Y, Feng J, et al. (2016) Preliminary treatment of bovine mastitis caused by *Staphylococcus aureus*, with trx-SA1, recombinant endolysin of *S. aureus* bacteriophage. *Veterinary Microbiology* 191: 65-71.
2. Marques VF, Motta CC, Soares BS, Melo DA, Coelho SMO, et al. (2016) Biofilm production and beta-lactamic resistance in Brazilian *Staphylococcus aureus* isolates from bovine mastitis. *Brazilian Journal of Microbiology* 1-7.
3. Eshete M, Bailey K, Nguyen TDT, Aryal S, Choi SO (2017) Interaction of Immune System Protein with PEGylated and Un-PEGylated Polymeric Nanoparticles. *Advances in Nanoparticles* 6: 103-113.
4. Dias DJS, Joanitti GA, Azevedo RB, Silva LP, Lunardi CN, Gomes AJ (2015) Chlorambucil Encapsulation into PLGA Nanoparticles and Cytotoxic Effects in Breast Cancer Cell. *Journal of Biophysical Chemistry* 6: 1-13.
5. Yuan XB, Yuan YB, Jiang W, Liu J, Tian EJ, et al. (2008) Preparation of rapamycin-loaded chitosan/PLA nanoparticles for immunosuppression in corneal transplantation. *International Journal of Pharmaceutics* 349: 241-248. 5/7
6. Liu W, Chen G, He G, He Z, Qian Z (2011) Sacrificial functional polystyrene template to prepare chitosan nanocapsules and in vitro drug release properties. *J Mater Sci* 46: 6758-6765.
7. Hamid ZAA, Tham CY, Ahmad Z (2018) Preparation and optimization of surface-engineered poly (lactic acid) microspheres as a drug delivery device. *J Mater Sci* 53: 4745-4758.
8. Agnihotri SA, Mallikarjuna NN, Aminabhavi TM (2004) Recent advances on chitosan-based micro- and nanoparticles in drug delivery. *Journal Control Release* 100: 5-28.
9. Chinh NT, Trang NTT, Thanh DTM, Hang TTX, Giang NV, et al. (2015) Thermal property, morphology, and hydrolysis ability of poly(lactic acid)/chitosan nanocomposites using polyethylene oxide. *Journal of Applied Polymer Science* 6-11.
10. Dev A, Binulal NS, Anitha A, Nair SV, Furuike T, et al. (2010) Preparation of poly (lactic acid)/chitosan nanoparticles for anti-HIV drug delivery applications. *Carbohydrate Polymers* 80: 833-838.
11. Wang W, Chen S, Zhang L, Wu X, Wang J, et al. (2015) Poly (lactic acid)/chitosan hybrid nanoparticles for controlled release of anticancer drug. *Materials Science and Engineering: C* 46: 514-520.
12. Mainardes RM (2007) Desenvolvimento de nanopartículas de PLA e PLA-PEG para administração intranasal de zidovudina. PhD Dissertation, Universidade Estadual Paulista.
13. Thi T, Nguyen T, Hee O, Seo J (2011) Coaxial electrospun poly (lactic acid)/chitosan (core/shell) composite nanofibers and their antibacterial activity. *Carbohydr Polym* 86: 1799-806.
14. Songsurang K, Suvannasara P, Phurat C, Puthong S (2013) Enhanced anti-topoisomerase II activity by mucoadhesive 4-CBS – chitosan/poly(lactic acid) nanoparticles. *Carbohydr Polym* 98: 1335-1342.
15. Jeevitha D, Amarnath K (2013) Chitosan/PLA nanoparticles as a novel carrier for the delivery of anthraquinone: Synthesis, characterization and in vitro cytotoxicity evaluation. *Colloids Surfaces B: Biointerfaces* 101: 126-134.
16. Rajan M, Raj V (2013) Formation and characterization of chitosan-poly(lactic acid)-poly(ethylene glycol)-gelatin nanoparticles: A novel biosystem for controlled drug delivery. *Carbohydr Polym* 98: 951-958.
17. Messai I, Lamalle D, Verrier B (2005) Poly (D, L-lactic acid) and chitosan complexes: interactions with plasmid DNA. *Colloids Surfaces A: Physicochem Eng Asp* 255: 65-72.
18. Lassalle V, Ferreira ML (2007) PLA Nano- and Microparticles for Drug Delivery: An Overview of the Methods of Preparation. *Macromol Biosci* 7: 767-783.
19. Frutos P, Torrado S, Perez-lorenzo ME, Frutos G (2000) A validated quantitative colorimetric assay for gentamicin. *J Pharm Biomed Anal* 21: 1149-1159.
20. Clinical and Laboratory Standards Institute (CLSI). Performance standards for antimicrobial disk susceptibility test; Approved Standard-Tenth Edition. Wayne, CLSI document M02-A10, 2009a.
21. Almeida E, Bona M De, Gisele F, Fruet TK, Cristina T, et al. (2014) Comparação de métodos para avaliação da atividade antimicrobiana e determinação da concentração inibitória mínima (CIM) de extratos vegetais aquosos e etanólicos. *Arq Inst Biol* 81: 218-225.
22. Hu Y, Jiang X, Ding Y, Ge H, Yuan Y, et al. (2002) Synthesis and characterization of Chitosan-poly(acrylic acid) nanoparticles. *Biomaterials* 23: 3193-3201.
23. Jones CF, Grainger DW (2009) In vitro assessments of nanomaterial toxicity. *Adv Drug Deliv Rev* 61: 438-456.
24. Watson P, Jones AT, Stephens DJ (2005) Intracellular trafficking pathways and drug delivery: fluorescence imaging of living and fixed cells. *Adv Drug Deliv Rev* 57: 43-61.
25. He C, Hu Y, Yin L, Tang C, Yin C (2010) Effects of particle size and surface charge on cellular uptake and biodistribution

- of polymeric nanoparticles. *Biomaterials* 31: 3657-3666.
26. Bradley AJ (2002) Bovine mastitis: an evolving disease. *Vet Journal* 164: 116-128.
 27. Rasal RM, Janorkar AV, Hirt DE (2010) Poly(lactic acid) modifications. *Prog Polym Sci* 35: 338-356.
 28. Vauthier C, Dubernet C, Fattal E, Pinto-alphandary H, Couvreur P (2003) Poly(alkylcyanoacrylates) as biodegradable materials for biomedical applications. *Adv Drug Deliv Rev* 55: 519-548.
 29. Liu P, Lo C, Chen C, Hsieh M, Huang C (2009) Use of Nanoparticles as Therapy for Methicillin-Resistant *Staphylococcus aureus* Infections. *Curr Drug Metab* 875-884.
 30. Carvalho FC, Chorilli M, Palmira M, Gremião D (2014) Plataformas Bio (Muco) Adesivas Poliméricas Baseadas em Nanotecnologia para Liberação Controlada de Fármacos-Propriedades, Metodologias e Aplicações. *Polímeros* 24: 203-213.
 31. Lyra MAM De, Soares-sobrinho JL, Brasileiro MT (2007) Sistemas Matriciais Hidrofilicos e Mucoadesivos para Liberação Controlada de Fármacos. *Lat Am J Pharm* 26: 784-793.
 32. Josué A, Laranjeira MCM, Fávère VT, Kimura IY, Pedrosa RC (2000) Liberação Controlada da Eosina Impregnada em Microesferas de Copolímero de Quitosana e Poli(ácido acrílico). *Polímeros Ciência e Tecnol* 10: 116-121.
 33. Wan Y, Wu H, Yu A, Wen D (2006) Biodegradable Polylactide/Chitosan Blend Membranes. *Biomacromolecules* 7: 1362-1372.
 34. Boo GA, Grijpma DW, Richards RG, Moriarty TF, Eglin D (2015) Preparation of gentamicin dioctyl sulfosuccinate loaded poly(trimethylene carbonate) matrices intended for the treatment of orthopaedic infections. *Clin Hemorheol Microcirc* 60: 89-98.
 35. Tripathi S, Mehrotra GK, Dutta PK (2009) Physicochemical and bioactivity of cross-linked chitosan-PVA film for food packaging applications. *Int J Biol Macromol* 45: 372-376.
 36. Bonilla J, Fortunati E, Vargas M, Chiralt A, Kenny JM (2013) Effects of chitosan on the physicochemical and antimicrobial properties of PLA films. *J Food Eng* 119: 236-243.
 37. Tam VH, Kabbara S, Vo G, Schilling AN, Coyle EA (2006) Comparative Pharmacodynamics of Gentamicin against *Staphylococcus aureus* and *Pseudomonas aeruginosa*. *Antimicrob Agents Chemother*, 50(8): 2626-31.

Copyright: ©2019 Karine Cappuccio de Castro, et al. This is an open-access article distributed under the terms of the Creative Commons Attribution License, which permits unrestricted use, distribution, and reproduction in any medium, provided the original author and source are credited.